ADVANCES IN ATMOSPHERIC SCIENCES, VOL. 28, NO. 3, 2011, 591–600

# Decadal Changes in Climatological Intraseasonal Fluctuation of Subseasonal Evolution of Summer Precipitation over the Korean Peninsula in the mid-1990s

WonMoo KIM*† [1], Jong-Ghap JHUN[1], Kyung-Ja HA[2], and Masahide KIMOTO[3]

[1] *School of Earth and Environmental Sciences/Research Institute of Oceanography, Seoul National University,* 151-742*, Korea*

[2] *Divison of Earth Environmental System, Pusan National University,* 609-735*, Korea*

[3] *Atmosphere and Ocean Research Institute, University of Tokyo,* 277-8564*, Japan*

(Received 10 March 2010; revised 18 June 2010)

**ABSTRACT**

Decadal changes in the subseasonal evolution and the phase-locked climatological intraseasonal fluctuation of summertime rainfall over the Korean Peninsula before and after the mid-1990s are investigated. The activity and the migration speed of the monsoon rain band over the East Asian region are altered in the recent decade, resulting in the drier conditions in late spring and the earlier onset of Changma. In early August when a climatological monsoon break was clear in the earlier decade, the precipitation has increased dramatically with a meridional coherency. The response to the enhanced convection over the South China Sea and southeastern China provides a favorable condition for more precipitation in early August through the changes in moisture transport and tropical cyclone passage.

**Key words**: decadal change, intraseasonal fluctuation, East Asian summer monsoon

**Citation**: Kim, W., J.-G. Jhun, K.-J. Ha, and M. Kimoto, 2011: Decadal changes in climatological intraseasonal fluctuation of subseasonal evolution of summer precipitation over the Korean Peninsula in the mid-1990s. *Adv. Atmos. Sci.*, **28**(3), 591–600, doi: 10.1007/s00376-010-0037-9.

## 1. Introduction

Asia-Pacific summer monsoon has three distinguishable regional sub-systems, i.e., the Indian summer monsoon (ISM), the western North Pacific summer monsoon (WNPSM), and the East Asian summer monsoon (EASM). Amongst the regional submonsoons, the East Asian summer monsoon is characterized by the poleward retreat in the late summer and east-west thermal contrast which tends to induce a zonal pressure gradient (Wang and LinHo, 2002). As a central part of the East Asian summer monsoon (EASM) region, the Korean Peninsula exhibits a typical mid-latitude monsoon rainfall structure in that the summer (June–August) precipitation accounts for more than 55% of the annual rainfall and the extended summer (May–September) precipitation is almost 75% of the annual total. The temporal distribution of summer precipitation over the northern EASM region exhibits two peaks (Ho and Kang, 1988), which are usually referred to as Changma (late June to mid July) and post-Changma (mid August to early September) rainfall in Korea. Studies on Chukwookee data (Jhun and Moon, 1997; Lim et al., 1996), a long-term rainfall measurement in Seoul, Korea, revealed the historical existence of the continuous rain period (Changma) from late June to July, a climatological monsoon "break" in early August, and a late-summer revival of precipitation between mid August and early September (Wang et al., 2007).

Also, there have been a number of studies concerning the climate regime shift over the EASM region including the Korean Peninsula. Wang et al. (2007) discussed the long-term variability of summer

*Corresponding author: WonMoo KIM, kwmski7@snu.ac.kr

†Current affiliation: Korea Ocean Research & Development Institute Ansan, 426-744, Korea

© China National Committee for International Association of Meteorology and Atmospheric Sciences (IAMAS), Institute of Atmospheric Physics (IAP) and Science Press and Springer-Verlag Berlin Heidelberg 2011

precipitation characters in Korea that onset and retreat dates tend to have the 180° out-of-phase relationship on multidecadal–centennial time scales, and the summit period has been delayed considerably from pentad 37 (P37, 30th June–4th July) of 1778–1807 to P44 (4th–8th August) of 1975–2004. Ha et al. (2005a) pointed out that the long-term variations of the summer monsoon rainfall over the Korean Peninsula are characterized by the change of summit period from late July in 1979–1992 regime to mid August in 1993–2001 regime. A recent study on summer rainfall over Korea (Kim and Suh, 2009) also detected the mid-1990 change (1995/1996) in heavy precipitation amounts and days by a Bayesian approach. Kwon et al. (2005) showed the regime shift of the summer mean circulation over the East Asian region and found a decadal change in relationship between EASM and WNPSM in the mid-1990s. They noted that the dominant factor controlling the EASM has changed from an ENSO-related variation in the earlier decade (1979–1993) to a WNPSM-dominated variation in the recent decade (1994–2004). In their further analysis, they coined one possible cause of this shift to the typhoon activity change over the South China Sea (SCS, Kwon et al., 2007).

As mentioned above, the time scales associated with the EASM variability span an extensive range from intraseasonal to decadal and each of them have been under intensive investigation. However, decadal changes in the intraseasonal structure are not well documented yet. This study examines the decadal variations in intraseasonal structures of the East Asian summer rainfall including the Korean Peninsula in the mid-1990s. In order to detect the statistically significant change point on the decadal time scale, we applied the Lepage test statistics (HK) to the 1-2-1 averaged precipitation data. The HK is a nonparameteric two-sample test that tests for the significant difference between the two samples, even if the distributions of the parent populations are unknown (Lepage, 1971; Yonetani and McCabe, 1994). As discussed in the following results, the major difference occurred in the mid-1990s and is comprised as (1) the faster northward migration of monsoon rain band during May to July, and (2) the significant rainfall increase in the early-August monsoon break period. To test the statistical existence of change in migration speed of the rain band, we define the precipitation gradient ($dP/dt$) as $dP$ = Pmax (maximum precipitation rate in P38–42)–Pmin (minimum precipitation rate in P27–33) and $dt$=Tmax (pentad which has maximum value in P38–42)–Tmin (pentad which has minimum value in P27–33) from 1-2-1 averaged precipitation data (61-station data collected by Korea Meteorological Administration, KMA). As can be seen in Fig. 1, the precipitation gradient ($dP/dt$) had undergone a statistically significant change in 1993/1994, and the P43–44 precipitation also changed in 1992/1993. Although they do not exactly match with each other, the change point was selected as 1993/1994 to separate 1979–1993 and 1994–2008 decades according to Kwon et al. (2005), when the large-scale circulation change is found over the EASM region. It was also found that this point was well distinguished by changes in convective activity over the SCS and southeastern China in midsummer. The difference in the subseasonal-scale temporal and spatial structure in summer precipitation between the two periods is shown and the related changes in the large-scale circulation field, convection, and tropical cyclones are investigated.

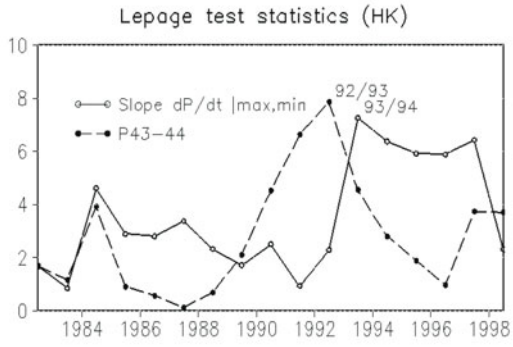


**Fig. 1.** Lepage test statistics (HK, $N$=10) of $dP/dt$ (solid line) and P43–44 precipitation rate (dashed line) calculated from 1-2-1 weighted average of KMA 61-station rainfall data. HK values exceeding 5.991 and 9.210 mean significant changes in statistics at 95% and 99% confidence levels.

## 2. Data and method

Daily rainfall records collected from 61 weather stations by KMA are converted to 5-day pentad (P12 always covering from 25th February to 1st March for both normal and leap years) mean. These 61 stations contain no missing values between 1971 and 2008. Also, the Climate Prediction Center (CPC) Merged Analysis of Precipitation (CMAP; Xie and Arkin, 1997) pentad data from 1979 to 2008 is utilized for further analysis.

As a proxy for convection, outgoing long-wave radiation (OLR; Liebmann and Smith, 1996) data produced by the National Oceanic and Atmospheric Administration/Climatic Diagnostics Center (NOAA/CDC) are used. Pentad mean sea surface temperature (SST) is calculated from the daily opti-

mum interpolation (OI) SST version 2. Pentad means of wind vector, geopotential height, and surface skin temperature are also calculated by the daily analyses of the National Centers for Environmental Prediction-Department of Energy (NCEP-DOE) Reanalysis 2 (NOAA_OI_SST_v2 and NCEP_Reanalysis 2 data provided by the NOAA/OAR/ESRL PSD, Boulder, Colorado, USA).

For the calculation of tropical cyclone (TC) passage and track density, the Regional Specialized Meteorological Center (RSMC) best track data are interpolated onto $2^\circ \times 2^\circ$ grid boxes. The same TC in one grid box is counted only once throughout their life time.

Decadal climate regimes are divided into two periods containing 15 years each, 1979–1993 and 1994–2008, respectively, according to Kwon et al. (2005). Differences between the two periods are tested by assuming Student's t-distribution of sample statistics.

## 3. Change in summer precipitation structure

Summer precipitation structure (Fig. 2c) shows two important aspects: There had been (1) a robust phase-locking of the intraseasonal fluctuation to the calendar date during 1979–1993 period and (2) a significant change in temporal distribution of rainfall over the Korean Peninsula in the mid-1990s. The precipitation rate is calculated from CMAP pentad by taking the area mean over 35°–40°N and 125°–130°E, and 1-2-1 averaging in time to smooth out the synoptic-scale variations. Annual mean rainfall rate over this region is 3.4±0.6 mm $d^{-1}$ (30-year mean ± standard deviation of interannual variation) and the summer-mean (June–August) value is 7.5±1.3 mm $d^{-1}$. It is interesting to note that the magnitude of the annual cycle is quite large (2.9 mm $d^{-1}$, calculated from the pentad mean), suggesting the existence of a strong monsoon climate in this region. Moreover, intraseasonal variability within the summer season still possesses a high value of standard deviation (2.4 mm $d^{-1}$, from pentad mean).

Before the mid-1990s, a remarkable phase-locking of the climatological intraseasonal fluctuation to the calendar date is evident, resulting in distinct Changma (P38–42, average rainfall rate=9.3±2.9 mm $d^{-1}$), post-Changma (P46–49, 9.4± 3.9 mm $d^{-1}$), and a climatological monsoon break (P43–45, 5.8±3.1 mm $d^{-1}$) in between. Before the onset of Changma there exists a dry period (P27–33, 3.3±1.2 mm $d^{-1}$). Such a phase-locking occurs quite regularly in that 10–11 years (the number of years when the precipitation rate is more (less) than the 15-year summer mean (7.2 mm $d^{-1}$) during Changma and post-Changma (break) periods) out of 15 exhibit typical Changma/break/post-Changma oscillation. In short, the climatological structure of summer rainfall over the Korean Peninsula does not show a smooth and continuous evolution but a strong intraseasonal-scale fluctuation. Changma precipitation is characterized as the results of low-level southwesterlies and low-level convergence (upper-level divergence) due to strong jet stream which work in association with the zonally elongated monsoon front. On the other hand, post-Changma rainfall develops from the combined effects of low-level moisture convergence under a strong upper-level jet, revival of a subtropical high, and typhoon activity (Seo and Byun, 2002). Monsoon break (P43–45) separates the two major rainy periods, resulting in two-peak subseasonal rainfall structures (Ha et al., 2005b).

The above-mentioned phase-locking dimmed after the mid-1990s. Only 6–8 years out of 15 show the typical phase-locking as mentioned above, and the oscillation period shortened to become a multi-peak structure. Before the commencement of the major rainy season, the Korean Peninsula suffers a stronger drought; however, the climatological onset of Changma occurs about 15 days earlier than before. As a result, the early July (P37) precipitation rate significantly increased from 6.8 mm $d^{-1}$ in the earlier decade to 11.0 mm $d^{-1}$ in the recent period. The most dramatic change can be found in the climatological monsoon break period, as the rainfall rate increased as much as 80% in the recent decade (from 5.8 mm $d^{-1}$ to 10.3 mm $d^{-1}$ in P43–44). The dominant period of the climatological intraseasonal fluctuation in the subseasonal evolution became shorter from 40–50 days to 20–30 days. Similar shortening of the oscillation period in other sub-monsoon regions is found by Kajikawa et al. (2009). They argued that the intraseasonal variability (ISV) period over the SCS has become shorter after the mid-1990s and that the merging of westward and eastward-moving disturbances which enhanced convective activity resulting in the prolonged period before the mid-1990s is lost in the recent decade, but exhibits a tilted band structure.

### 3.1 *Decrease in* P32 *and increase in* P37

In the early and middle part of summer (May–July), the zonally elongated monsoon rain band, meiyu/Baiu, dominates the regional precipitation structure in the EASM region. Climatologically, meiyu/Baiu initiates in May around 20°N and migrates northward through June to July. This northward movement of the rain band slows down while passing around 30°N. Such northward movement of the rain band shows clear phase-locking to the calendar date (LinHo and Wang, 2002). Figure 2 shows the climatological northward migration of the rain band which is

averaged over 120°–130°E and its difference between the two periods (1994–2008 minus 1979–1993). The phase speed of the climatological northward propagation of the rain band is about 12° month$^{-1}$ up to 30°N, but it slows down to about 6° month$^{-1}$ in the mid-latitude. To the north and south of this rain band occur dry zones. The western flank of the North Pacific subtropical high (NPSH, which is associated with the southern dry zone) separates the East Asian monsoon mei-yu/Baiu system from the intertropical convergence zone (ITCZ), and the moisture transports from ISM region, southern hemisphere, and western North Pacific merge into the SCS and South China. Thus, the dry zones and the rain band are dynamically-related phenomena.

After the mid-1990s (Fig. 2b), the speed of the northward movement of CISO over the East Asian region became faster, resulting in the stronger spring drought and the earlier onset of Changma in Korea.

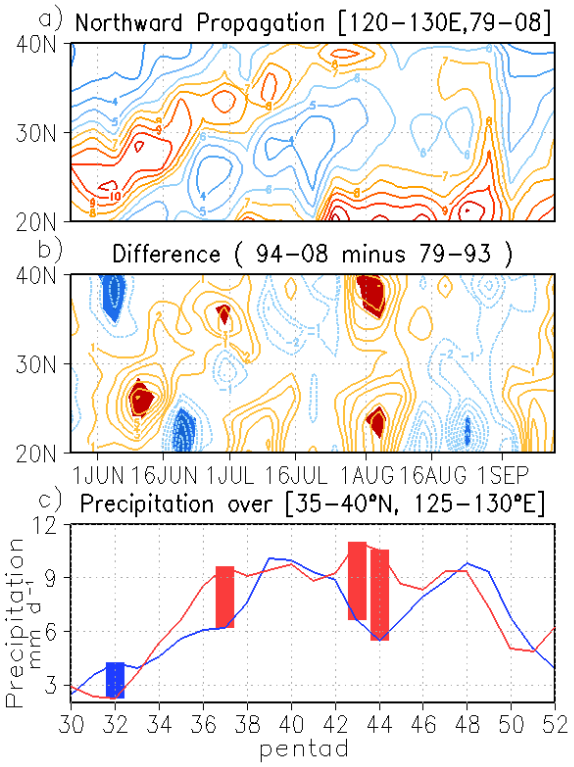


**Fig. 2.** (a) Climatological northward movement of precipitation rate (mm d$^{-1}$) averaged over 120°–130°E for the whole period (1979–2008). (b) Difference between 1979–1993 and 1994–2008. Shaded areas indicate significant changes at 95% confidence level. (c) 1-2-1 smoothed climatological rainfall for 1979–1993 (blue) and 1994–2008 (red) periods. Marked with bars are the statistically significant changes between the two periods at 95% confidence level.

The difference of the rain band between the two periods marks a 14° month$^{-1}$ slope and the maximum axis of difference passes through the line of climatological propagation. Also, north and southward of the maximum axis of difference occur intensified dry phases. By making a scrutiny into the climatological subseasonal evolution structure during the early part of the summer (P32–37) reveals that the monsoon rain band intensity is significantly stronger during P32–P35 and dry anomalies are located to the north of the maximum rain band during P32–33 and to the south during P35–37 (Figures not shown). Overall picture shows the strengthened rain band system and the accelerated northward propagation during June to early July. The decrease (increase) in P32 (P37) rainfall results from the change in a well-organized monsoon front and its northward migration.

To confirm the robustness of the change, we performed the principal component (empirical orthogonal functions) analysis (EOF/PCA) on normalized precipitation over the East Asian region for the extended summer (P25–50, May to early September; The use of covariance matrix rather than correlation matrix yield a similar result, but we apply EOF/PCA on the latter to eliminate the inherent weighting over the tropical regions and give an emphasis on the northern part of the East Asian region). Figures 3a–c show the loading vectors and corresponding time series. Solid lines in the time series indicate a 15-year-mean time evolution of the given principal components, while dashed lines show ±1 interannual standard deviation from the mean value. The time series are normalized, but the spatial patterns retain their variances and the unit is mm d$^{-1}$. Figure 3d shows the peak time of principal modes in action. The lower (upper) end of the yellow bar indicate the pentad when the leading mode has its minimum (maximum) value, while the red square implies the time when the 2nd mode reaches its maximum. Thus the combination of the yellow bar and the red square implies the initiation, peak, and termination of the migration mode. The red and blue bars on the top of Fig. 3d show the pentads when the 3rd mode reaches its maximum in late summer. First two (1st and 2nd) leading modes explain 20% of the total variance and have quadratic relationships to each other, representing the northward movement of the rain band. They have a strong phase-locking character that the 1st mode reaches its minimum (maximum) value between late-May to early-June (late-June to early-July) and the 2nd mode peaks its maximum during the middle of June. As seen from the standard deviation (dashed) lines, they are well phase-locked and have statistically significant values during their peak stages. In a recent period, i.e., 1994–2008, the

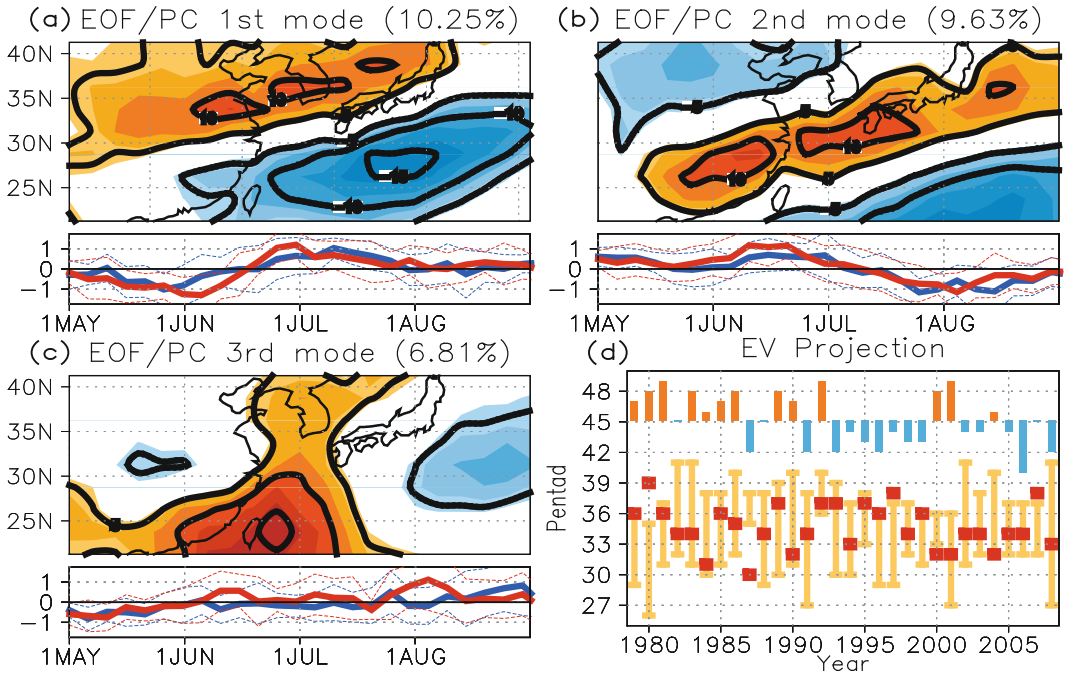


**Fig. 3.** (a–c) Empirical orthogonal functions and their corresponding time series calculated from P25–50 precipitation rate for each year over 20°–40°N, 100°–150°E region. Solid lines in the time series are 15-year mean principal components and dashed lines indicate ± 1 interannual standard deviation from the mean. Blue (red) lines are 15-year mean values of 1979–1993 (1994–2008) period. (d) Pentad when maximum/minimum projection values occur for 1-2-1 averaged time series of each (1st–3rd) mode. For the 1st mode (yellow bars), lower (upper) ends indicate the pentad when the leading mode has its minimum (maximum) value. The red (blue) squares denote the pentad when the 2nd (3rd) mode has its maximum value.

phase-locking of the migration (1st and 2nd) modes is strengthened and the northward-moving speed is accelerated. During the 1979–1993 period, the minimum value of the leading mode occurred in late-May and the maximum value in early- to mid-July. After the mid-1990s, however, they occurred in early-June and late-June, respectively. The time between the occurrence of the minimum and the maximum values of the leading mode was about 39 days in 1979–1993, but it has significantly shortened (at the 95% confidence level) to 31 days in the recent decade. The stronger drought in P32 and earlier onset of Changma (P37) are described by the change in the two leading modes which explain about 20% of the total variability. The 3rd mode, which still posses a high percentage of total variance (about 7%), however, exhibits a completely different structure and behavior. It generally reaches its maximum value in August and resembles the north-south coherency found in the difference pattern in early August (P43–44).

Since the precipitation data contain large temporal and spatial variances and high degrees of freedom, it is hard to obtain a small number of sets (modes) which can explain most of the variability. In such a case, comparing the results with other variables and giving a possible physical explanation for the mathematical modes would ensure the robustness of the principal components. It turned out that the two leading modes of precipitation jointly show the migration of the rain band system as described above, and the leading principal components (PCs) of low-level circulation field are highly correlated with the migration modes. The 1st (33.1%), 2nd (27.1%), and 3rd (8.4%) modes of 850 hPa zonal wind over the same region are significantly correlated with the 2nd (correlation coefficient, $r$=0.62), 1st ($r$=0.63), and 3rd ($r$=0.53) modes of precipitation principal components, respectively. Also, the PCs of 1st (49.4%), 2nd (22.0%), and 3rd (9.3%) modes for the normalized 500 hPa geopotential height have a correlation coefficient of 0.51, 0.53, and 0.51 with corresponding PCs of precipitation, respectively (figures not shown). Spatial distribution of precipitation and low-level circulation (Fig. 4) in the selected periods [P32 (June 5th–9th), P37 (June 30th–July 4th) and P43–44 (July 30th–August 8th)] also reveals the different structures between early-June decrease/early-July increase and early-August change. These particular pentads are selected as the following

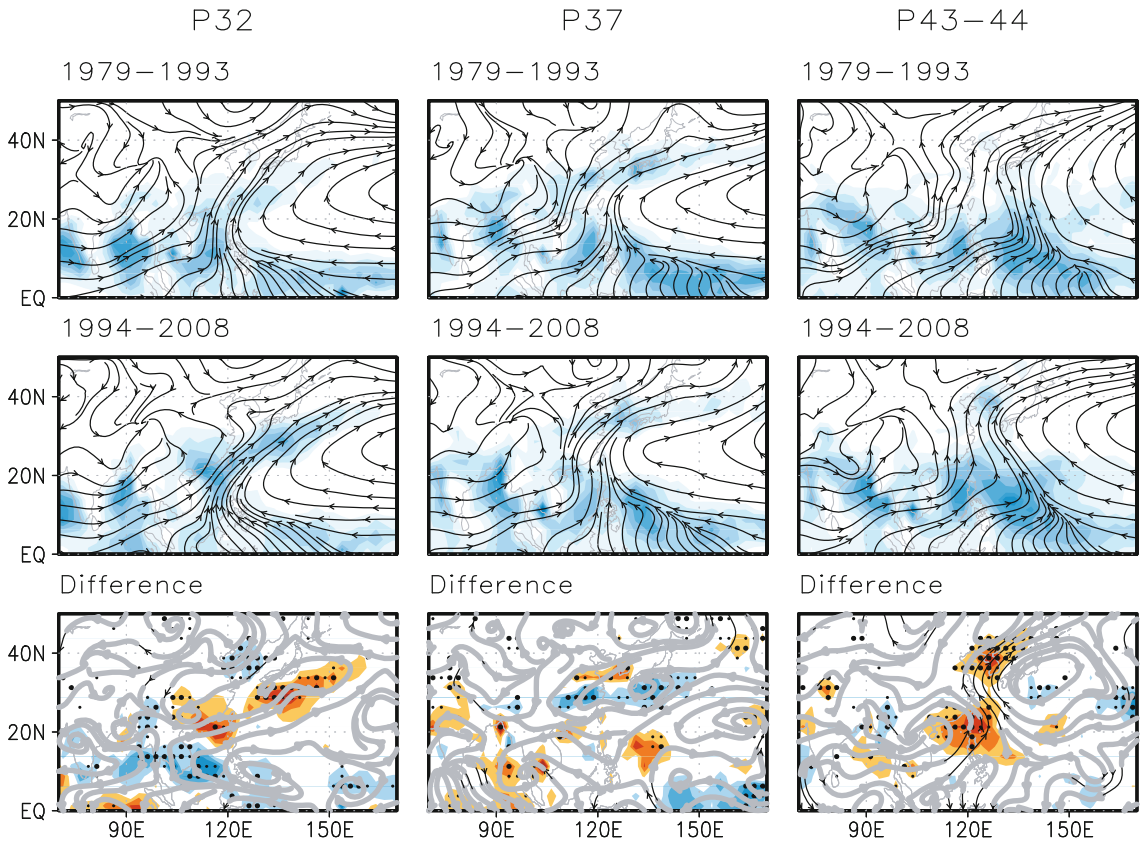


**Fig. 4.** Pentad mean climatology of precipitation (shadings) and low level (850 hPa) circulation (streamlines) for 1979–1993 (upper) and 1994–2008 (middle), and difference between the two periods (lower) for P32 (left), P37 (middle), and P43–44 mean (right). In the difference maps, statistically significant changes with 95% confidence level are denoted by dots (precipitation) and black lines (circulation).

reasons: (1) P32 and P37: During P32 through P37, it is clear that the monsoon rain band is intensified in the recent period and is located southward (northward) to the previous position in P32–33 (P35–37), resulting in a faster northward migration. (2) P43–44: Late-July to early-August was a climatological monsoon break period in Korea before the mid-1990s, but the rainfall rate significantly increases (about 80%) after the mid-1990s in this period. Upper and middle panels show the 15-year climatological rainfall rate (shadings) and streamlines, while lower panels show the difference between the two periods. Large- (small-) dotted areas in the difference map indicate statistically significant changes in precipitation at the 95% (90%) confidence level and darker segments of the streamlines imply significant changes in wind vectors. In P32, the overall intensity of the mei-yu/Baiu rain band is much stronger in the recent period; however, rainfalls over the Korean Peninsula, Indochina, and tropics are significantly reduced. Stronger anticyclonic flow over the yellow sea hinders the rain band reaching the northern part of the EASM region, but induces stronger confluent flow into the monsoon front, consequently strengthening the mei-yu/Biau rain band. At the same time, the Korean Peninsula, located northward of the rain band, experiences drier condition due to the stronger anticyclonic flow in recent periods.

A similar zonal structure of change but with opposite signs is shown in P37. The monsoon rain band intensity is somewhat weaker, but to the north of the band exist a small increase in rainfall rate. With the expansion of the North Pacific high to the north and northwestward, moisture fluxes from the ISM, the WNPSM, and the southern hemisphere merge into the narrow zone of the WPSH flank and intensify the Changma rainfall. Both periods are under the influence of a strong monsoon front and spatial patterns of change in precipitation have a well organized zonal structure related to the rain band, which is, again, related to the faster northward migration of the monsoon front.

### 3.2 *Increased precipitation in the climatological monsoon break season* (P43–44)

A significant increase of rainfall in early August (P43–44) is, however, manifested by a different mech-

anism which is concurrent with enhanced precipitation over the SCS. Unlike early to midsummer (May–July) when the climatological precipitation structure is zonally elongated in association with the monsoon rain band, in early-August (P43–44) the spatial structure of change is completely different from the above: it shows a meridionally coherent pattern, rather than the rain band-related zonal structure, with significant increase in precipitation over the SCS and over the Korean Peninsula (Fig. 2b and Fig. 4). In the 1979–1993 period, the western edge of the North Pacific high resides to the east of 130°E and the moisture flux from the ISM region does not clearly merge into the southerly flow around it. However, after the mid-1990s, the North Pacific high expanded to the northern EASM region inducing strong confluent southerlies toward the Korean Peninsula. The moisture fluxes from ISM, warm pool, and WNP regions converge into the southerly flow over the EASM region. As a result, the precipitation over the Korean Peninsula during the monsoon break season has increased as much as 80% in recent period. The second maximum of change occurs in the SCS sector. Interestingly, the change in convective activity or precipitation over the SCS leads that over the Korean Peninsula about 5 days (e.g., Fig. 2). The phase-locking of the 3rd principal mode (Fig. 3c) also confirms this south-north coherent change. During 1979–1993 period, this phase-locking is insignificant throughout the summer (significant phase-locking occur only in May but with negative sign). After the mid-1990s, however, the 3rd mode became an essential part of climatological evolution of the summer precipitation and exhibits a significant phase-locking in early-August. The 15-year mean value of the 3rd mode in P43–44 changed from $-0.2\pm0.5$ to $1.0\pm0.9$. Also, the time when maximum projection of the 3rd mode occurs shifted from P46 in 1979–1993 period to P44 in 1994–2008 period (Fig. 3d).

Figure 5 shows the difference in P42–44 outgoing long-wave radiation (OLR) between the two periods and the time series of area-averaged OLR over SCS (15°–22.5°N, 110°–120°E). The southwest-northeast tilted convection anomaly pattern over Southeast Asia is clear and the suppressed convection is identified over the southern hemispheric counterpart. The time mean of area-averaged OLR in 1979–1993 regime is $230\pm16$ W m$^{-2}$, but it decreases abruptly and significantly to $210\pm19$ W m$^{-2}$ in the recent (1994–2008) period. The convective activity over the SCS has generally increased throughout summer (Kwon et al., 2007); however, on a sub-seasonal scale, it is significant only in P42–44 at the 95% confidence level. Considering the large spatial scale of the change in OLR, this shift of convection activity could be a result of change in large-scale CISO, the phase-locking of ISOs. Among the Asian sub-monsoon regions, SCS suffers the greatest phase difference between the two periods during summer and fall, and the EASM region also experiences the change in phase as well as amplitude of CISO (figures not shown). It has also been reported that the intraseasonal variability (ISV) over the SCS has undergone a decadal change in the mid-1990s, i.e., the dominant period of individual ISOs has been shortened (from 64 days in 1979–1993 to 42 days in 1994–2007; Kajikawa et al., 2009). Another important factor that should be taken into account is the change in TC passage into the SCS region in these particular pentads. In 1979–1993, only 6 TCs (0.4 yr$^{-1}$) passed through SCS (15°–22.5°N, 110°–120°E) during P42–44, while in recent period the number of TCs increased to 13 (0.9 yr$^{-1}$, figure not shown). A recent paper on TC tracks (Chen et al., 2009) documented the impact of a large scale ISV in the WNP region, but the small number of samples obstructed detecting a direct linkage between above-mentioned change and the large-scale westerly/easterly characters. The change of typhoon tracks seems to be partly due to the westward shift of

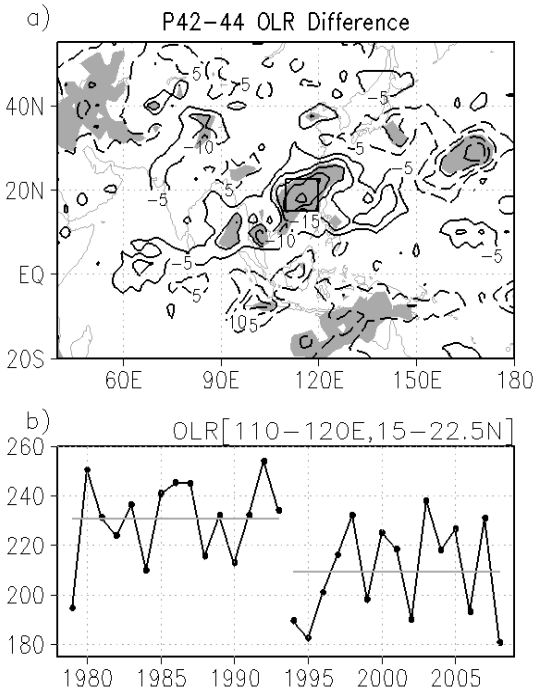


**Fig. 5.** (a) P42–44 mean OLR (W m$^{-2}$) difference between the two periods (1994–2008 minus 1979–1993). Shaded areas indicate the statistically significant change at 95% confidence level. (b) Time series of area-averaged OLR over 15°–22.5°N, 110°–120°E [boxed area in (a)] and time mean of each period (1979–1993 and 1994–2008).

major typhoon formation regions associated with a warmer sea surface temperature in the SCS (Ho et al., 2004) in recent years and the change in oscillatory periods of subtropical intraseasonal variability.

The enhanced convective activity over the SCS can influence the East Asian climate through a barotropic response (Kwon et al., 2005). Figure 6 shows the P43–44 mean climatological position of geopotential height (GPH) of 5880 m at 500 hPa for each period and differences in low-level (850 hPa) moisture fluxes between the two periods. The 15-year mean contour of 5880 m clearly shows the expansion of the WNPSH to the East Asian region in the recent period. Also, alternating cyclonic (centered at 20°N, 110°E, and 45°N, 175°E) and anticyclonic (centered at 35°N, 145°E) wave-like trails are obvious in the low-level flow. This pattern emanates from the SCS region where the strong and abrupt change of convective activity is detected, and the response pattern is barotropic in structure in the mid-latitude. As the southerly flow intensifies in the 120°–130°E region, moisture transports from two major sources, the Indian Ocean and the Western Pacific Ocean (Lim et al., 2002), increased after the mid-1990s due to this wave trail pattern. The enhanced moisture fluxes converge over the Korean Peninsula to the south of the entrance of the strong upper-level jet stream, resulting in an anomalous rainfall in the monsoon break season (P43–44) of Korea.

For a supplementary mechanism, since the structure of response is barotropic in the mid-latitude, the deep-layer-mean environmental flow (Ho et al., 2004) or the mid-tropospheric flow can serve as steering flows of mid-latitude TC passage to a good approximation. Although the 500-hPa height anomaly (area averaged over 25°–35°N, 135°–150°E) posses a strong interannual variability (figure not shown), the western flank of the subtropical North Pacific high extends more to the west about 25° (as represented by the 5880-m GPH contours, from 150°E to 125°E) in recent periods, and this intensification of the 500-hPa height anomaly is significant only in the P36 and P43–44 during the summer. The number of TCs passing the area around the Korean Peninsula (30°–40°N, 110°–130°E) in the monsoon break season did not change significantly (12 and 11 in each 15-year period of 1979–1993 and 1994–2008, respectively), but their tracks did (Fig. 7). With the westward expansion of the North Pacific subtropical high, TC passages in recent periods have become more recurving; TC track densities eastward of 130°E and southward of 40°N have decreased, while those westward of 130°E have increased significantly.

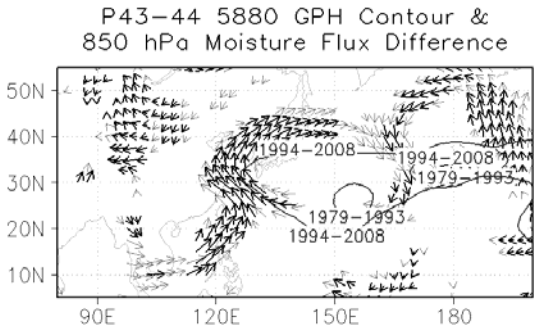


**Fig. 6.** P43–44 mean climatological position of geopotential height contours of 5880 m at 500 hPa for 1979–1993 and 1994–2008 periods. Vectors show the difference of 850 hPa moisture fluxes between the two periods. Only statistically significant changes in moisture flux are denoted by light and bold arrows, which indicate 90% and 95% confidence levels, respectively.

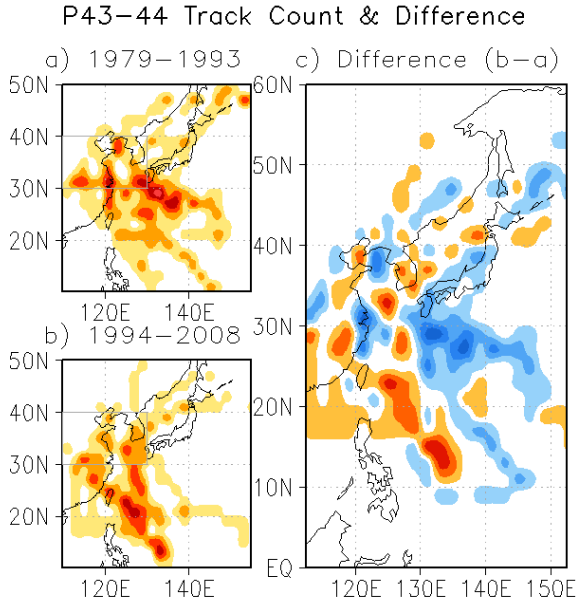


**Fig. 7.** The track density (a and b) in each period and their difference (c) of TCs that pass through 30°–40°N, 110°–130°E region during P43–44. The red (blue) areas in (c) denote the increase (decrease) of the TC track density. Track density is calculated from RSMC best track interpolated into 2°×2° longitude-latitude grid box. The same TCs are counted only once in each grid box.

## 4. Summary and discussion

During the mid-1990s, climatological intraseasonal fluctuation of the subseasonal evolution of summer precipitation over the Korean Peninsula has undergone a regime shift. Changes that occurred after the mid-1990s are characterized as:

(1) the strong early-summer drought in P32 and in-

creased rainfall in P37 (earlier onset of Changma) due to the strong monsoon frontal activity and the faster northward migration of the rain band and

(2) the significant increase in precipitation rate during climatological monsoon break season (P43–44) with a meridional coherency.

The overall picture shows the shorter climatological intraseasonal fluctuation period from 40–50 days in the 1979–1993 regime to 20–30 days in the 1994–2008 regime. In the late spring-early summer, changes in precipitation have a zonally oriented structure, and are the result of the activity and the migration speed of the monsoon rain band. On the other hand, early-August change is induced by the stronger convective activity over the SCS and South China through enhanced moisture fluxes (and their convergence) into the EASM region, and recurving TC pathways.

Increased TC passage into the SCS and South China seems to be the primary cause of intensive convection; however, another signal comes from the Indian summer monsoon sector. The upper-level divergence (low-level convergence) and mid-tropospheric vertical motion are greatly reduced in the western coast of India from mid-July to mid-August after the mid-1990s. The magnitude decreases to less than 1/4∼1/5 of the mean value of the earlier decade (Fig. 8). This dramatic change in circulation may induce a teleconnection pattern all the way through the SCS region (figure not shown), or rather directly influence the EASM by affecting the Rossby wave train across the Eurasian continent (Ding and Wang, 2007); however, the change point is 1992/1993 rather than 1993/1994 and the interpretation of the mechanism needs more analysis.

It has been documented that many other factors can influence the summer monsoon over the EASM region, e.g., a land-sea thermal contrast (Cheng et al., 2008), Indian summer monsoon activity through an upper-level teleconnection (Ding and Wang, 2005), western North Pacific summer monsoon (WNPSM; Wang and LinHo, 2002), thermal and hydrological forcing of the Tibetan plateau (Zhang et al., 2004; Zhao et al., 2007), El Niño-Southern Oscillation (ENSO), and etc. Difference in P42–44 sea surface temperature between 1979–1993 and 1994–2008 (figure not shown) also confirms the recent warming trend in these particular pentads: A horseshoe-shaped warming over the western Pacific is obvious with the strongest warming occurring in the Kuroshio extension and South Pacific convergence zone (SPCZ) regions. Secondary maxima of the warming can be found in the south Indian Ocean and over the warm pool. Li et al. (2008) found that the warming in the tropical Indian Ocean can enhance the EASM using multiple AGCMs: The tropical Indian Ocean basin warming consistently

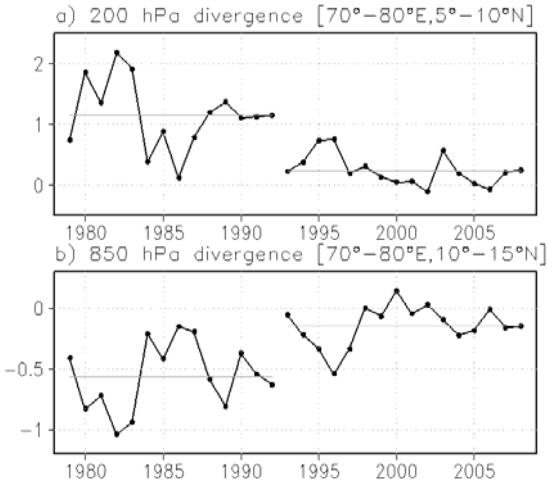


**Fig. 8.** (a) 200 hPa and (b) 850 hPa divergence ($10^5$ $s^{-1}$) over the western coast of India in P40–47. Straight lines indicate mean values for 1979–1992 and 1993–2008 periods. Differences are statistically significant at 99% confidence level.

induces an intensified southwesterly flow to East China (lower-level) and stronger South Asian high (upper-level), both of which favor the enhancement of the EASM. We also found a meaningful relationship between the basin-wide Indian Ocean warming and the P43–44 increase in precipitation over the Korean Peninsula, i.e., the June–July Indian Ocean SST is significantly correlated with the P43–44 rainfall ($r$=0.47). On the other hand, change in the warm pool region may affect the EASM (Ding, 2004), but the effects on a sub-seasonal time scale is not well understood. Furthermore, the land-sea thermal contrast seems to contribute little to the P43–44 increase in precipitation over the Korean Peninsula (figure not shown). Also, there have been intensive studies on the effect of spring snow cover over the Tibetan Plateau on EASM and its decadal change (e.g., Zhang et al., 2004). These aspects require further analysis and are left for a future study.

***Acknowledgements.*** This work was funded by the Korea Meteorological Administration (KMA) Research and Development Program under Grant CATER 2006-4205 and by BK21 program. Partial support for M. Kimoto was given by the Innovative Program of Climate Change for the 21st Century of the Japanese Ministry of Education, Culture, Sports, Science and Technology.

## REFERENCES

Chen, T.-C., S.-Y. Wang, M.-C. Yen, and A. J. Clark, 2009: Impact of the intraseasonal variability of the

western North Pacific large-scale circulation on tropical cyclone tracks. *Wea. Forecasting*, **24**, 646–666.

Cheng, H., T. Wu, and W. Dong, 2008: Thermal contrast between the middle-latitude Asian continent and adjacent ocean and its connection to the East Asian summer precipitation. *J. Climate*, **21**, 4992–5007.

Ding, Q., and B. Wang, 2005: Circumglobal teleconnection in the northern hemisphere summer. *J. Climate*, **18**, 3483–3505.

Ding, Q., and B. Wang, 2007: Intraseasonal teleconnection between the summer Eurasian wave train and the Indian monsoon. *J. Climate*, **20**, 3751–3767.

Ding, Y., 2004: Seasonal march of the East Asian summer monsoon. *East Asian Monsoon*, C.-P. Chang, Ed., Mainland Press, 3–53.

Ha, K.-J., S.-K. Park, and K.-Y. Kim, 2005a: On interannual characteristics of Climate Prediction Center merged analysis precipitation over the Korean peninsula during the summer monsoon season. *Int. J. Climatol.*, **25**, 99–116.

Ha, K.-J., K.-S. Yun, J.-G. Jhun, and C.-K. Park, 2005b: Definition of onset/retreat and intensity of Changma during the boreal summer monsoon season. *Journal of the Korean Meteorological Society*, **41**, 927–942.

Ho, C.-H., and I.-S. Kang, 1988: The variability of precipitation in Korea. *Journal of the Korean Meteorological Society*, **24**, 38–48.

Ho, C.-H., J.-J. Baik, J.-H. Kim, D.-Y. Gong, and C.-H. Sui, 2004: Interdecadal changes in summertime typhoon tracks. *J. Climate*, **17**, 1767–1776.

Jhun, J.-G., and B.-K. Moon, 1997: Restorations and analyses of rainfall amount observed by Chukwookee. *Journal of the Korean Meteorological Society*, **33**, 691–707.

Kajikawa, Y., T. Yasunari, and B. Wang, 2009: Decadal change in intraseasonal variability over the South China Sea. *Geophys. Res. Lett.*, **36**, L06810.

Kim, C., and M.-S. Suh, 2009: Change-point and change pattern of precipitation characteristics using Bayesian method over South Korea from 1954 to 2007. *Journal of the Korean Meteorological Society*, **19**, 199–211.

Kwon, M., J.-G. Jhun, B. Wang, S.-I. An, and J.-S. Kug, 2005: Decadal change in relationship between east Asian and WNP summer monsoons. *Geophys. Res. Lett.*, **32**, L16709.

Kwon, M., J.-G. Jhun, and K.-J. Ha, 2007: Decadal change in east Asian summer monsoon circulation in the mid-1990s. *Geophys. Res. Lett.*, **34**, L21706.

Lepage, Y., 1971: A combination of Wilcoxon's and Ansari-Bradley's statistics. *Biometrika*, **58**, 213–217.

Li, S., J. Lu, G. Huang, and K. Hu, 2008: Tropical Indian Ocean basin warming and East Asian summer monsoon: A multiple AGCM study. *J. Climate*, **21**, 6080–6088.

Liebmann, B., and C. A. Smith, 1996: Description of a complete (interpolated) outgoing longwave radiation dataset. *Bull. Amer. Meteor. Soc.*, **77**, 1275–1277.

Lim, K.-H., J.-G. Jhun, and J.-H. Oh, 1996: Assessment of climatological precipitation amount in the Korean peninsula in terms of the precipitation records of Korean rain gauge and precipitation model output (in Korean). S. N. U. Department of Atmospheric Sciences, Rep. KOSEF 93-0700-06-02-3, Ed., 165pp.

Lim, Y.-K., K.-Y. Kim, and H.-S. Lee, 2002: Temporal and spatial evolution of the Asian summer monsoon in the seasonal cycle of synoptic fields. *J. Climate*, **15**, 3630–3644.

LinHo, and B. Wang, 2002: The time-space structure of the Asian-Pacific summer monsoon: A fast annual cycle view. *J. Climate*, **15**, 2001–2019.

Seo, D.-I., and H.-R. Byun, 2002: Period and mechanism of summer/Autumn rainy season in Korean peninsula. *J. Kor. Meteor. Soc.*, **12**, 402–405.

Wang, B., and LinHo, 2002: Rainy season of the Asian-Pacific summer monsoon. *J. Climate*, **15**, 386–398.

Wang, B., J. G. Jhun, and B. K. Moon, 2007: Variability and singularity of Seoul, South Korea, rainy season (1778–2004). *J. Climate*, **20**, 2572–2580.

Xie, P. P., and P. A. Arkin, 1997: Global precipitation: A 17-year monthly analysis based on gauge observations, satellite estimates, and numerical model outputs. *Bull. Amer. Meteor. Soc.*, **78**, 2539–2558.

Yonetani, T., and G. McCabe Jr., 1994: Abrupt changes in regional temperature in the conterminous United States, 1895–1989. *Climate Res.*, **4**, 13–23.

Zhang, Y., T. Li, and B. Wang, 2004: Decadal change of the spring snow depth over the Tibetan Plateau: The associated circulation and Influence on the East Asian summer monsoon. *J. Climate*, **17**, 2780–2793.

Zhao, P., Z. Zhou, and J. Liu, 2007: Variability of Tibetan spring snow and its associations with the hemispheric extratropical circulation and East Asian summer monsoon rainfall: An observational investigation. *J. Climate*, **20**, 3942–3955.